Composites: Part B 43 (2012) 3491–3496

Contents lists available at SciVerse ScienceDirect

Composites: Part B

journal homepage: www.elsevier.com/locate/compositesb

Multiscale molecular modeling of SWCNTs/epoxy resin composites mechanical behaviour

Mariana Ionita *

University Politehnica of Bucharest, 132 Calea Grivitei, 010737 Bucharest, Romania

ARTICLE INFO

Article history:
Received 27 September 2011
Received in revised form 2 December 2011
Accepted 23 December 2011
Available online 2 January 2012

Keywords:
C. Computational modeling
B. Mechanical properties
B. Thermal properties
Epoxy resin/SWCNTs composites

ABSTRACT

Atomistic and mesoscale simulations were conducted to estimate the effect of the diameter and weight fraction of single walled carbon nanotubes (SWCNTs) on mechanical behaviour and glass transition temperature (T_g) of SWCNTs reinforced epoxy resin composites. Atomistic periodic systems of epoxy resin and epoxy resin/SWCNTs were built with different weight ratios and were subject of an extensive multistage equilibration procedure. Molecular dynamics simulations were used to estimate glass transition temperature, Young modulus and solubility parameter of epoxy resin and epoxy resin/SWCNTs composites. Dissipative particle dynamics method and Flory–Huggins theory was employed to predict epoxy resin/SWCNTs morphologies. The results show that incorporation of SWCNTs with diameters ranging from 10 to 14 Å has beneficial effect on mechanical integrity and T_g. Overall, the agreement between predicted material properties and experimental data in the literature is very satisfactory.

1. Introduction

Due to their excellent physical, chemical and mechanical properties carbon nanotubes (CNTs) [1] continue to be one of the hottest research areas and are considered to be highly potential nanofillers to improve the polymers properties [2]. There has been much speculation as the excellent properties of the CNTs may be transferred to the polymer composites just by combining the right choice of base materials with the suitable CNTs amount and appropriate processing method [3–6]. Carbon nanotubes dispersion within polymer matrix is another important challenge given their natural tendency to aggregate due to inter-molecular van der Waals interactions. For successful dispersion a strong binding between the polymer and the carbon nanotubes that can overcome strong van der Waals interactions between the tubes themselves is required [7]. On the base of van der Waals interactions recent studies indicated that polymers show the ability to discriminate between carbon nanotube species in terms of either diameter or chiral angle [8]. Maiti et al. investigated the effect of single walled carbon nanotubes (SWCNTs) diameter on the material morphology. Based on solubility parameter he explains why poly(methyl methacrylate) mixes well with SWCNTs of diameter close to 1.4 nm, *i.e.* SWCNTs (10,10) but not with SWCNTs (15,15), diameter $\sim$ 1.9 nm, and why poly(m-phenylenevinylene-co-2,5-dioctyloxy-*p*-phenylenevinylene) shows selective affinity to SWCNTs of diameter $\sim$ 1.5 nm [9,10]. Efficient dispersion and possibly the alignment of CNTs within a matrix is difficult to control and design experimentally conversely, computationally molecular modeling can provide such crucial insights [7,9]. The prediction of the CNTs dispersion and alignment within polymer matrices would allow for the rational decisional process for the definition of new and improved composite materials and would limit the efforts of synthetic chemists in following the inefficient Edisonian prescription of creating all possible mixtures in order to isolate the desired material. Computational molecular modeling at atomistic and mesoscale has been demonstrated to accurately reproduce mechanical behaviour, solubility parameters and material morphology [7,9,11–14]. However a reliable quantitative description at atomistic and mesoscale for a composite polymer/CNTs is rather challenging because of the significant number of atoms involved, large equilibration times and the very complex chemical network structure which might present practical difficulties when attempting to simulate their properties in a realistic fashion. Previously we have reported atomistic simulations of epoxy resin/SWCNTs composite system but this first foray was not successful due to approximation of some features of the real material [15]. Our previous experience in this area has led us to adopt a policy of ensuring that the computational models represent as accurately as possible the real network, relying on experimental data such as, cross-linking degree of the polymer, density of the real material, number of repeated units within the polymer chains *etc.* Up to now, however, there are very few works reporting the computational characterization of epoxy resin/SWCNTs composites and to the best of my

* Tel.: +40 740465637.
E-mail address: mariana.ionita@polimi.it

1359-8368/$ - see front matter © 2012 Elsevier Ltd. All rights reserved.
doi:10.1016/j.compositesb.2011.12.008

knowledge no computational work assessed the effect of the diameter of SWCNTs on mechanical properties or the morphologies of SWCNTs reinforced epoxy resin composites [15–17].

Epoxy resins are actually finding broad applications in a variety of industries, medicine, household and are also important bulk structural materials for aerospace projects [17]. Their mechanical properties are of relevance for all upper mentioned applications consequently, numerous studies are focused on improving epoxy materials properties using nanofillers such as CNTs able to improve or/and to impart new properties [17]. However, questions concerning the appropriate type of CNTs, *e.g.* SWCNTs, double-walled CNTs (DWCNTs) or multi-walled CNTs (MWCNTs), and the relevance of a surface functionalisation are still to be answered [16–18].

The aim of this work was to define a modeling recipe based on (i) forcefield based atomistic simulation to predict the glass transition temperature, mechanical behaviour of composite materials epoxy resin/SWCNTs with different diameters and further to derive solubility parameters values among all system components; (ii) mapping of solubility parameters values onto mesoscale simulation parameters; (iii) mesoscale simulations to determine composite systems morphologies.

2. Computational methodology

The molecular models construction and subsequent simulations were conducted using the Materials Studio 5.0 molecular modeling package of Accelrys and the COMPASS forcefield [19]. The non-bond interactions (van der Waals and electronic static forces) within a cutoff distance of 9.5 Å were considered.

2.1. Construction of the computational bulk models

Single repeated unit of epoxy resin, *i.e.* diglycidyl ether of bisphenol A, has been manually constructed and minimized in order to obtain a stable starting structure. Conversely, the SWCNTs with different diameters, SWCNTs (4,4) (diameter $\sim$ 5 Å), SWCNTs (8,8) (diameter $\sim$ 10 Å) and SWCNTs (10,10) (diameter $\sim$ 14 Å) and 4.92 Å axial length are available as standard model in software data base. The axial length of carbon nanotubes was reduced in order to diminish the computational cost. Charge groups have been assigned to fragments of each repeated unit and SWCNTs. The isolated epoxy chain configurations consisting of 11 monomers were then generated starting from the repeated units using Build Polymer tool of the software. Computational bulk models of epoxy resin, epoxy resin/SWCNTs (4,4), epoxy resin/SWCNTs (8,8) and epoxy resin/SWCNTs (10,10) were implemented with 91:9 and 95:5 weight ratios under periodic boundary conditions employing the Amorphous cell module based on Theodorou and Suter [20] packing technique. This allows us to determine both the effect of SWCNTs diameter and relative composition on the mechanical behaviour and glass transition temperature. In order to simulate the cross-linking process the epoxy resin chains and the curing agent, ethylene tetra-amine, were manually linked together by breaking and forming the appropriate bonds. The main features of the computational systems, number of atoms and polymer chains, density, dimension, are listed in Table 1. Since the systems contain aromatic elements the packing stage was performed for all the models at a very low initial density, 0.01 g/cm^3 [21].

2.2. Equilibration of the computational bulk models

The initial packing models were subject to an extensive multistage equilibration procedure composed of a sequence of energy minimisation and constant number of molecules, pressure and temperature (NPT) and constant number of molecules, volume and temperature (NVT)-molecular dynamics (MD) simulations with forcefield parameters and annealing [21,22]. A first equilibration cycle consisted of five steps of energy minimisation and MD simulations in which conformation and non-bonded pair interaction terms in the forcefield have been scaled down, by scaling factors from 0.01 to 1 [21,22]. Each step of minimisation was performed using two different algorithms: initially Steepest descent algorithm was used since it is an extremely robust method most likely to generate a lower-energy structure, generally applied for the first 10–1000 steps of minimisation. Afterwards, the most advanced Conjugate gradient–Fletcher–Reeves algorithm was used to achieve efficient convergence to the minimum. The energy convergence criterion was to meet at derivative of less than 0.001 kcal mol^{-1}. Each step of NVT-MD simulation runs for 300,000 steps and the time step was 1 fs. The Berendsen thermostat was used to control the temperature. After this equilibration cycle each packing model was subject of a short MD-NPT, simulation at p = 1 GPa and T = 300 K for about 5000 steps in order to compress the model and to reach the density of the real material. The Berendsen barostat was used to control the pressure during NPT-MD simulations. After the compression stage the systems present a certain degree of unrealistic tension which indicates that the packing models need further equilibration. The equilibration cycle consisting of five steps of MM and MD calculations each

Table 1
Main characteristics of the computational systems.

Model name	Model composition (w/w)	Total no. of atoms within the model	No. of atoms of SWCNTs	No. of atoms of epoxy resin	Model density (g/cm^3)	Model length (Å)	Elastic modulus (GPa)	Poisson's ratio
Epoxy resin	100	4590	–	4590	1.061	36.79	3.58 ± 0.22	0.28
Epoxy resin/ SWCNTs (4,4)	95/5	4654	128	4526	1.103	36.90	3.86 ± 0.50	0.30
Epoxy resin/ SWCNTs (4,4)	91/9	4782	210	4572	1.152	38.30	5.21 ± 0.32	0.29
Epoxy resin/ SWCNTs (8,8)	95/5	4718	128	4590	1.106	36.94	4.43 ± 0.48	0.33
Epoxy resin/ SWCNTs (8,8)	91/9	4846	192	4654	1.167	36.75	5.95 ± 0.47	0.29
Epoxy resin/ SWCNTs (10,10)	95/5	4750	160	4590	1.114	36.87	6.12 ± 0.85	0.27
Epoxy resin/ SWCNTs (10,10)	91/9	4830	240	4590	1.158	36.88	7.51 ± 0.39	0.33

From Ref. [31] the density of epoxy resin is 1.06 g/cm^3. From Ref. [2] the density of SWCNTs is 2.1 g/cm^3. Densities were calculated by the weight average of epoxy resin and SWCNTs.

one characterised by scaling factors was coupled with annealing technique which consists of a sequence of NVT-MD simulations at 750 K, 600 K, 450 K, and 300 K each one for 300 ps to further equilibrate the computational systems. The equilibration routine was repeated until computational bulk model reached the density of the real material and total energy and temperature reached stable values during MD calculations. The overall simulation time requested for the equilibration procedure for each of the models was of about 8 ns.

2.3. Assessment of mechanical properties, glass transition temperature and morphology of computational bulk models

Discover Analysis tool, which uses a static approach originating in the work of Theodorou and Suter [20] was used to describe mechanical behaviour of epoxy resin and epoxy resin/SWCNTs composite systems. Thus, for each of the computational systems virtual uniaxial traction tests along the *x*, *y*, and *z* perpendicular edges were performed and Young moduli along these directions were calculated. Afterwards, the Young modulus of the epoxy resin and epoxy resin/SWCNTs composite systems was calculated by taking the average value in the *x*, *y*, and *z* directions. A more detailed description of these methods is given elsewhere [23].

MD-NPT simulations were conducted to predict glass transition temperature (T_g) by monitoring changes in cell density. MD simulations started from 440 K under a pressure of 0.1 MPa. Temperature was decreased with a rate of 10 °C/200 ps and was controlled with Berendsen thermostat. Each subsequent simulation was started from the final configuration obtained at the previous temperature. The MD simulations were performed with a step of 1 fs. Changes in computational bulk model density were plotted against the entire working range of temperature.

Amorphous Cell analysis module was further employed to predict solubility parameter, δ, of epoxy resin using the Scatchard and Hildebrand theoretical treatments of mixing [24,25]. A collection of solubility parameters for SWCNTs with different diameters, calculated by Maiti and co-workers employing atomistic molecular modeling, are available in the literature [9]. Afterwards Flory Huggins theory and dissipative particle dynamics (DPD) mesoscale technique [26,27] was used to estimate the dispersability of SWCNTs with different diameters within epoxy resin matrices. DPD provides a dynamics algorithm for studying coarse-grained systems over long length and time scales. In DPD calculations a small region of material (group of atoms) is represented by a single bead, therefore the number of particles to be simulated is reduced with respect to atomistic simulations. The beads mutually interact via soft potentials. Three forces are acting between each pair of nonbonded beads: a conservative force, F_{ij}^C, interaction which is linear in the bead–bead separation, a dissipative force, F_{ij}^D, representing the viscous drag between moving beads, and a random force, F_{ij}^R, representing stochastic impulse. The nonbonded interactions between a pair of nonbonded beads can be written as:

$$f_i = \sum_{i \neq j} (F_{ij}^C + F_{ij}^D + F_{ij}^R) \quad (1)$$

Groot and Warren established a link between the conservative force and the Flory–Huggins interaction parameter, χ, which is a measure of the compatibility of binary mixtures. Flory–Huggins interaction parameters were calculated using the following equation [28].

$$\chi_{ij} = \frac{(\delta_i - \delta_j)^2 V}{RT} \quad (2)$$

where δ_i and δ_j, are the solubility parameters of *i* and *j* species, *V* is a reference volume, taken to be the mean molar volume of the two beads (SWCNTs and epoxy resin beads), while *R* is universal gas constant, and *T* is temperature. Subsequently, Flory–Huggins parameters were converted into repulsion parameters (a_{ij}) between pairs of beads using Eq. (3) and their values are listed in Table 2.

$$a_{ij} = \frac{\chi}{0.306} + 25 \quad (3)$$

Table 2
Solubility, Flory–Huggins and repulsion parameters for system components.

Species	δ (J cm^3)$^{1/2}$	χ_{ij}	a_{ij}
Epoxy resin	18.60	0	25.0
SWCNTs (4,4)	28[a]	29	54
SWCNTs (8,8)	20[a]	0.65	25.65
SWCNTs (10,10)	19[a]	0.05	25.05

[a] From Ref. [9].

In addition, there is also a harmonic force between bonded beads. Bonded beads interact by Hookean springs controlling the bonds stretching and angles bending. A single spring constant is used to specify the average bonded interactions. All forces are short-ranged with a fixed cut-off radius, r_c, set as unit length.

In present study an epoxy resin monomer, diglycidyl ether of bisphenol A, is represented with a single bead. The considered epoxy resin chains consisted of 11 beads. For SWCNTs mesoscale model seven aromatic rings were represented with a bead. SWCNTs with different diameters, SWCNTs (4,4) (diameter $\sim$ 5 Å), SWCNTs (8,8) (diameter $\sim$ 10 Å) and SWCNTs (10,10) (diameter $\sim$ 14 Å) and 100 Å length were implemented. Computational cubic bulk models of epoxy resin/SWCNTs (4, 4), epoxy resin/SWCNTs (8, 8) and epoxy resin-SWCNT (10, 10) were implemented with different compositions 91:9 and 95:5 (w/w) within a simulation box of $20 \times 20 \times 20$ consisting of $2.4 \times 10{,}000$ beads. The beads of the same molecule are connected by harmonic spring having the spring constant $c = 4$. The DPD calculations run over 2×10^5 steps with a time step of 0.05 reduced units (r.u.). As Groot and Warren suggested density of the system was set to $\rho = 3$ r.u. [27].

3. Results and discussion

The methodology adopted in the present work couples atomistic and mesoscale computational techniques in order to get more exhaustive insights on epoxy resin and epoxy resin/SWCNTs (4,4), epoxy resin/SWCNTs (8,8) and epoxy resin/SWCNTs (10,10) composite systems properties. The present simulation work is focused on composite systems with large SWCNTs weight fraction (5 wt.% and 9 wt.%). Although experimental systems typically contain much lower weight fraction of CNTs, the simulation results can help to make useful prediction for lower SWCNTs weight fraction enhancement effect by extrapolation.

The equilibration routine allows the obtainment of stable periodic cells in which SWCNTs and cured epoxy resin chains are placed randomly in non-overlapping positions. Fig. 1 is a snapshot of the last MD simulation step for the model epoxy resin/SWCNTs (8,8) (91:9 w/w).

3.1. Prediction of mechanical properties

A first investigation of the computational bulk models it considers the mechanical behaviour. Models were subject of virtual uniaxial tests along three perpendicular directions further Young moduli and Poisson ratios of epoxy resin and epoxy resin/SWCNTs composite systems were calculated and are listed in Table 1. These values are taken from the average of the three configuration runs for a given set of parameter values. Young modulus values are positive and Poisson ratios are consistent with the theory of linear elasticity; hence, mechanical stability of the material was achieved. Poisson ratio values ranging from 0.29 to 0.33 is indicating that the

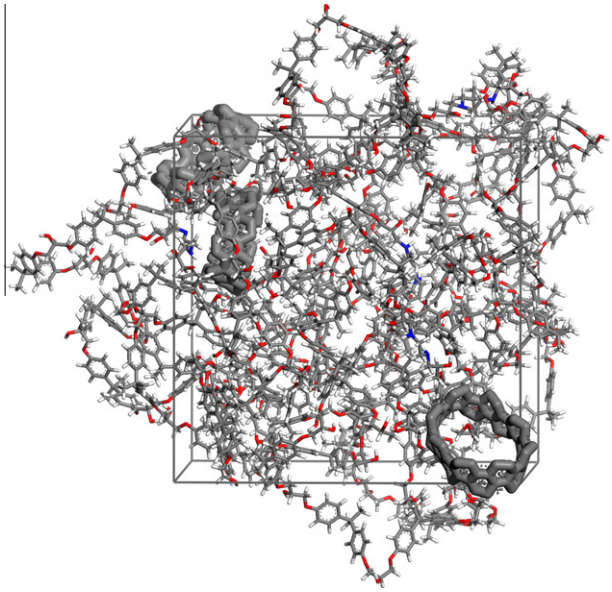

Fig. 1. Computational bulk model of epoxy resin/SWCNTs (8,8) (91/9 w/w) after the equilibration procedure.

composites epoxy resin/SWCNTs are rigid materials. Generally a reinforcement of the epoxy resin was observed with the addition of the SWCNTs. The reinforcement was related on the one hand to the SWCNTs amount and on the other hand to the SWCNTs diameter. Higher values of SWCNTs percentage cause an increase of materials stiffness, this effect is evident for SWCNTs fraction of about 5 wt.%. Doubling the SWCNTs content (from 5 wt.% to 9 wt.%) the values of Young's modulus significantly increase particularly for epoxy resin/SWCMTs (8, 8) and epoxy resin/SWCNTs (10, 10) composite systems. Conversely the Young moduli were related to the material components as depicted in Table 1. The maximal value of Young's modulus (7.51 GPa) was obtained for the composite system epoxy resin/SWCNTs (10, 10) (91:9 w/w) thus we can conclude that the best reinforcement of epoxy resin is produced by SWCNTs (10, 10). Similar reinforcement extent was observed by adding the SWCNTs (8,8) instead by adding the SWCNTs (4,4) just a marginal effect was observed. The difference in the reinforcing efficiency between SWCNTs (4,4), SWCNTs (8,8) and SWCNTs (10, 10) is most likely due to different interfacial adhesion (intermolecular forces) between SWCNTs and epoxy resin chains. Similar trend was found in the work of Gojny and co-workers [29,30]. They observed an efficient stress transfer from epoxy matrix to the tubes just in the case of a good interfacial adhesion between the CNTs and epoxy matrix. Interfacial adhesion quality was estimated assuming Flory–Huggins theory on the base of solubility parameters [26]. The solubility parameter values for systems components are depicted in Table 2. Flory–Huggins theory predicts that components with similar δ values lead to small repulsions, accordingly epoxy resin ($\delta = 18.60\ (J/cm^3)^{-0.5}$) should present a good adhesion with SWCNTs (8,8) ($\delta = 20\ (J/cm^3)^{-0.5}$) and SWCNTs (10, 10) ($\delta = 19\ (J/cm^3)^{-0.5}$). In contrast, SWCNTs (4,4) which exhibits a significantly different δ value ($\delta = 29\ (J/cm^3)^{-0.5}$) is expected to present high repulsion toward epoxy resin, therefore a poor adhesion and tendency to agglomerate.

The numerical Young modulus value for epoxy resin is in good agreement with theoretical and experimental results from the literature which range from 3.43 to 3.75 GPa [31,32]. The predicted Young's modulus values for epoxy resin/SWCNTs composite systems compare well with recent experimental measurements from the literature. Li et al. studied epoxy resin/SWCNTs and measured an increase of the modulus from 4 to 7 GPa with addition of 5 wt.% of SWCNTs [33]. The calculated Young modulus values of epoxy resin/SWCNTs are slightly higher than the values reported in the literature. This small difference between the predicted and experimental values can be attributed to the larger weight fraction of SWCNTs considered and to the low imperfections density of the models. In real material, it is most likely that a certain amount of the material presents imperfections which are not fully taking into account the idealised situation stipulated in the atomistic simulation.

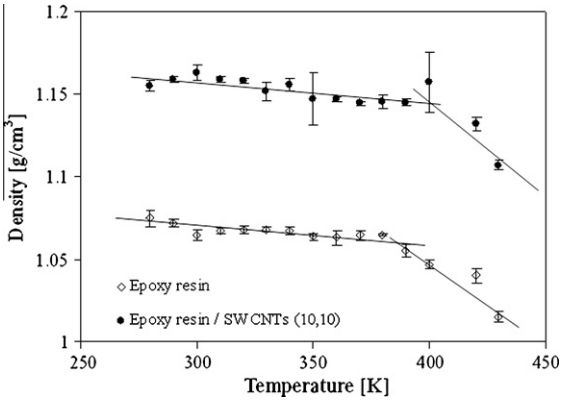

Fig. 2. Changes in unit cell density of epoxy resin and epoxy resin/SWCNTs (10,10) (91/9 w/w) with temperature.

3.2. Glass transition temperature

Molecular dynamics simulations were employed to predict the changes in density against the temperature for epoxy resin and epoxy resin/SWCNTs (10,10) (91/9 w/w) computational bulk models. For both a steady increase of the density with decreasing temperature followed by a clear change in the density slope curve was observed (Fig. 2). The abrupt change in the density slope curve defines the value of glass transition temperature at approximately 110 °C for epoxy resin and at approximately 125 °C for epoxy resin/SWCNTs (10,10). The glass transition temperature of the epoxy resin/SWCNTs (10,10) is 15 °C higher than that of pristine resin. The significant increase of T_g was attributed to an adequate SWCNTs (10,10) dispersion and strong SWCNTs (10,10)/epoxy resin interfacial interactions which constrain the polymer chains mobility. Both increases and decreases in the T_g have been reported in the literature dependant upon the dispersion and interaction between the matrix and the filler [17,28]. Sangermano and co-workers observed that the increase of T_g of CNTs/epoxy resin depends on the CNTs dispersion and interfacial interaction. Their studies have revealed an increase of epoxy resin T_g, with 9–13 °C with the addition of SWCNTs [34]. The predicted T_g value for epoxy resin is very close to the experimental $T_g = 105$ °C [31] and predicted $T_g = 109$ °C [30] values found in the literature.

3.3. Prediction of SWCNTs dispersion within computational systems

In order to analyze the SWCNTs dispersion homogeneity within epoxy resin/SWCNTs composite systems with different compositions DPD mesoscale simulation technique was employed. Fig. 3 illustrates the morphology of the three composite systems after 2×10^5 DPD calculation steps. At the beginning of the calculation all the components were mixed together, after 10,000 steps SWCNT (4,4) congregate, as expected according to Flory–Huggins theory [25]. As the simulation time increases the formation of SWCNTs (4,4) domains was observed for both system compositions 91:9 and 95:5 (w/w). SWCNTs (8,8) and SWCNTs (10,10)

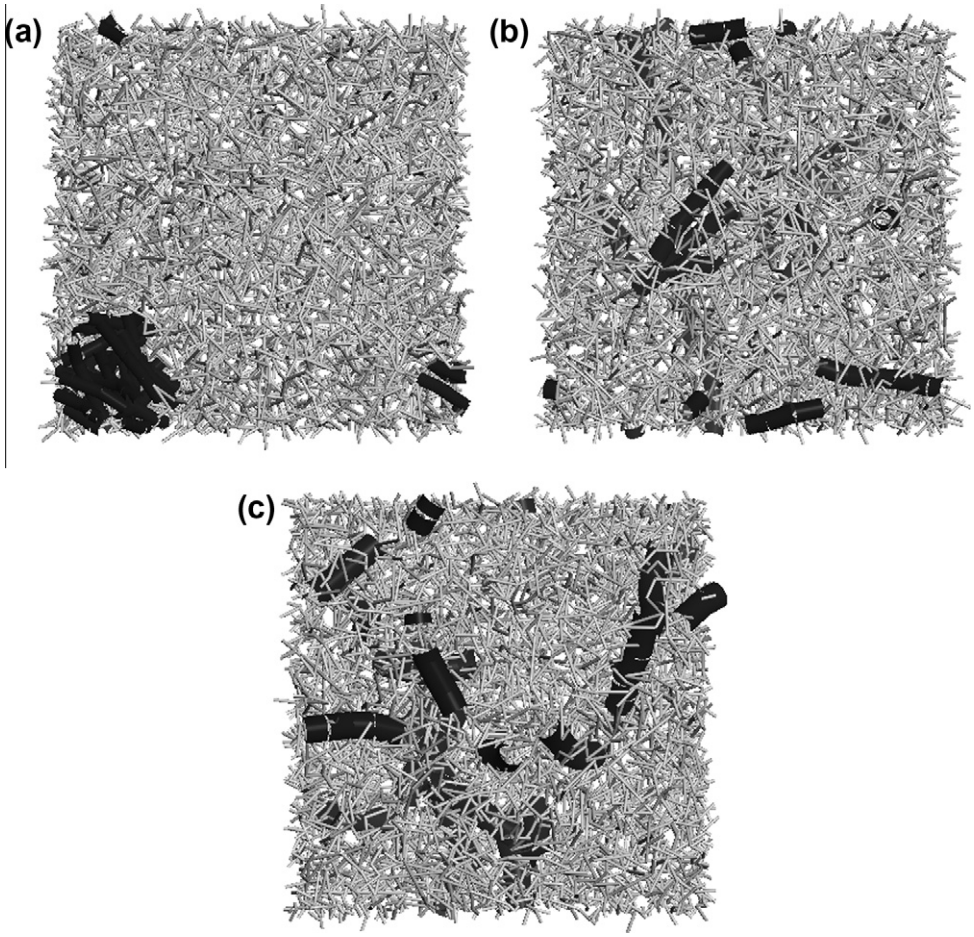

Fig. 3. Equilibrium morphology of epoxy resin/SWCNTs (4,4) (95/5 w/w) (a), epoxy resin/SWCNTs (8,8) (91/9 w/w) (b) and epoxy resin/SWCNTs (10,10) (91/9 w/w) (c) systems as modelled by DPD. SWCNTs are shown in black and epoxy chains are shown in light grey.

mix well with epoxy resin polymer chains. From Fig. 3b and c, it can be easily observed that SWCNTs (8,8) and (10,10) are well embedded into the epoxy matrix and singularly dispersed regardless of their concentration. Therefore, the improvement of mechanical properties and T_g observed by means of atomistic molecular modeling is reasonable.

Uniform dispersion of carbon nanotubes in the epoxy resin is a fundamental challenge. The effective utilization of SWCNTs in composite applications strongly depends on the ability to homogeneously disperse them throughout the epoxy resin matrix. The methodology adopted in the present work couples atomistic and mesoscale computational techniques in order to get more exhaustive insight on materials morphology and how this influence physical properties of materials. Within this perspective, adjoining computational modeling to the necessary experimental activity adds more insight on the molecular phenomena that take place at the nanoscale, and possibly helps the experimentalists in conducting more focused and model-oriented tests avoiding the time-consuming approach based on the trial-and-error procedure.

4. Conclusions

This work confirms that MM, MD and DPD computational tools allow to achieve well equilibrated bulk models and to predict epoxy resin and epoxy resin/SWCNTs composite material properties accurately.

The simulation results suggested that SWCNTs (10,10) and SWCNTs (8,8) are properly dispersed within the epoxy resin matrix and have beneficial effect on mechanical integrity and T_g. Instead incorporation of SWCNTs (4,4) generates just a marginal effect on mechanical behaviour due to weak interfacial adhesion with epoxy resin chains and their tendency to agglomerate.

The maximal value of Young modulus (7.51 GPa) was obtained for the composite system epoxy resin/SWCNTs (10,10) (91:9 w/w) thus can be concluded that the best reinforcement of epoxy resin is produced by SWCNTs (10,10).

The simulation results indicate that incorporation of SWCNTs (10,10) at 9 wt.% in the epoxy matrix lead to an increase of T_g with about 15 °C.

The prediction of epoxy resin/SWCNTs composite properties priori to laboratory design can help to conduct more focused and model oriented investigations, avoiding the time consuming trial and error approach.

Acknowledgement

Authors recognise financial support from the European Social Fund through POSDRU/89/1.5/S/54785 project: Postdoctoral Program for Advanced Research in the field of nanomaterials.

References

[1] Bogani L, Wernsdorfer W. A perspective on combining molecular nanomagnets and carbon nanotube electronics. Inorg Chim Acta 2008;361:3807–19.
[2] Kang I, Heung YY, Kim JH, Lee JW, Gollapudi R, Subramaniam S, et al. Introduction to carbon nanotube and nanofiber smart materials. Comp Part B: Eng 2006;37:382–94.

[3] Thostenson ET, Chou TW. Aligned multi-walled carbon nanotube reinforced composites: processing and mechanical characterization. J Phys D: Appl Phys 2002;35:77–80.
[4] Suhr J, Koratkar N, Keblinski P, Ajayan P. Viscoelasticity in carbon nanotube composites. Nat Mater 2005;4:134–7.
[5] Branzoi V, Branzoi F, Pilan L. Electrochemical fabrication and capacitance of composite films of carbon nanotubes and polyaniline. Surf Interface Anal 2010;42:1266–70.
[6] Lau AKT, Hui D. The revolutionary creation of new advanced materials—carbon nanotube composites. Comp Part B: Eng 2002;33:263–77.
[7] Panhuis M, Maiti A, Dalton AB, Nort A, Coleman JN, McCarthy B, et al. Selective interaction in a polymer−single-wall carbon nanotube composite. J Phys Chem B 2003;107:478–82.
[8] Nish A, Hwang J-Y, Doing J, Nicholas RJ. Highly selective dispersion of single-walled carbon nanotubes using aromatic polymers. Nature Nanotechnol 2007;2:640–6.
[9] Maiti A, Wescott J, Kung P. Nanotube-polymer composites: insights from Flory–Huggins theory and mesoscale simulations. Mol Sim 2005;31:143–9.
[10] Nyden MR, Stoliarov SI. Highly selective dispersion of single-walled carbon nanotubes using aromatic polymers. Polymer 2008;21:635–41.
[11] Clancy TC, Frankland SJV, Hinkley JA, Gates TS. Molecular modeling for calculation of mechanical properties of epoxies with moisture ingress. Polymer 2009;50:2736–42.
[12] Gautieri A, Ionita M, Silvestri D, Votta E, Vesentini S, Fiore GB, et al. Computer-aided molecular modeling and experimental validation of water permeability properties in biosynthetic materials. J Comput Theor Nanosci 2010;7:1287–93.
[13] Aprodu I, Soncini M, Montevecchi FM, Redaelli A. Mechanical characterization of actomyosin complex by molecular mechanics simulations. J Appl Biomat Biomech 2010;8(1):20–7.
[14] Pruna A, Ionita M. Polypyrrole/carbon nanotube composites: molecular modeling and experimental investigation as anti-corrosive coating. Prog Org Coat 2011;72:647–52.
[15] Ionita M, Damian CM. Molecular modeling for calculation of mechanical properties of SWCNTs/epoxy resin composites: effect of SWCNTs diameter. Mat Plast 2011;48:54–7.
[16] Gou J, Fan B, Song G, Khan A. Study of affinities between single-walled nanotube and epoxy resin using molecular dynamics simulation. Int J Nanosci 2006;5:131–44.
[17] Gojny FH, Wichmann MHG, Fiedler B, Schulte K. Influence of different carbon nanotubes on the mechanical properties of epoxy matrix composites – a comparative study. Comp Scie Technol 2005;65:2300–13.
[18] Zhu J, Kim JD, Peng H, Margrave JL, Khabashesku VN, Barrera EV. Improving the dispersion and integration of single-walled carbon nanotubes in epoxy composites through functionalization. Nano Lett 2003;3:1107–13.
[19] Sun H. COMPASS: an ab initio force–field optimized for condensed-phase applications - overview with details on alkane and benzene compounds. J Phys Chem B 1998;102:7338–64.
[20] Theodorou DN, Suter UW. Atomistic modeling of mechanical properties of polymeric glasses. Macromolecules 1986;19:139–54.
[21] Hofmann D, Fritz L, Ulbrich C, Schepeers C, Bohning M. Detailed-atomistic molecular modeling of small molecule diffusion and solution processes in polymeric membrane materials. Macromol Theory Simul 2000;9:293–327.
[22] Tocci E, Hofman D, Paul D, Russo N, Drioli E. A molecular simulation study on gas diffusion in a dense poly(ether–ether–ketone) membrane. Polymer 2001;42:521–33.
[23] Ionita M. Molecular modeling for calculation of mechanical properties of polyaniline–carbon naotubes. In: ASME 2010 10th biennial conference on engineering systems design and analysis, vol. 4. ESDA 2010; 2010. p. 139–46.
[24] Scatchard G. Equilibria in non-electrolyte solutions in relation to the vapor pressures and densities of the components. Chem Rev 1931;8:321–33.
[25] Hildebrand JH. Solubility. J Am Chem Soc 1916;38:1452–73.
[26] Rouse PE. The theory of nonlinear viscoelastic properties of diluted solutions for scaling polymers. J Chem Phys 1953;21:1273–80.
[27] Materials Studio 5.0 software (Accelerys, Inc. UK) tutorial.
[28] Groot RD, Warren PB. Dissipative particle dynamics: bridging the gap between atomistic and mesoscopic simulation. J Chem Phys 1997;107:4423–35.
[29] Gojny FH, Wichmann MHG, Kopke U, Fiedler B, Schulte K. Carbon nanotube-reinforced epoxy-composites – enhanced stiffness and fracture toughness at low nanotube content. Comp Sci Technol 2004;64:2303–8.
[30] Frankland SJV, Caglar A, Brenner DW, Griebel M. Molecular simulation of the influence of chemical cross-links on the shear strength of carbon nanotube–polymer interfaces. J Phys Chem B 2002;106:3046–8.
[31] Fan HB, Yuen MMF. Material properties of the cross-linked epoxy resin compound predicted by molecular dynamics simulation. Polymer 2007;48:2174–8.
[32] <http://www.resin.com/resin/am/pdf/SC0772.pdf>; 2005.
[33] Li XD, Gao SH, Scrivens WA, Fei DL, Xu XY, Sutton MA, et al. Nanomechanical characterization of single-walled carbon nanotube reinforced epoxy composites. Nanotechnology 2004;15:1416–23.
[34] Sangermano M, Borella E, Priola A, Messori M, Taurino R, Potschke P. Use of single-wall carbon nanotubes as reinforcing filler in UV curable epoxy system. Macromol Mater Eng 2008;293:708–13.